Microgels Loaded with Gold Nanorods: Photothermally Triggered Volume Transitions under Physiological Conditions†

Mallika Das, Nicolas Sanson, Daniele Fava, and Eugenia Kumacheva*

Department of Chemistry, University of Toronto, 80 Saint George Street, Toronto, ON M5S 3H6, Canada

Received June 2, 2006. In Final Form: September 1, 2006

Photothermally driven volume transitions in polymer microgels have promising applications for site-specific drug delivery and photodynamic therapy. We studied the temperature-induced volume phase transitions for a series of thermoresponsive microgels of various compositions to find a system with a sharp transition in the physiologically relevant range spanning 38−41 °C in 0.01 M phosphate-buffered saline solution (pH = 7.4). We found that the poly(*N*-isopropylacrylamide-maleic acid) microgels showed an 8-fold decrease in size under the aforementioned conditions. These microgels were loaded with gold nanorods designed to absorb in the near-IR spectral range. Following irradiation at λ = 809 nm, the microgels underwent a large, reversible, photothermally triggered change in volume. We believe that this microgel system is a promising candidate for photothermally controlled drug release.

Introduction

Microgels have a vast range of applications stemming from their facile synthesis and stimuli-responsive volume transitions.[1] The controlled delivery of drugs from microgels is one such area: pH, thermal, and photothermal triggers or biological stimuli (e.g., interactions with enzymes and proteins) can lead to large changes in the volume of microgel drug carriers, which trigger the release of drugs from the particles.[2] Furthermore, microgels can be bioconjugated with specific molecules that recognize receptors on specific cells and can then be used for site-specific drug delivery.[3,4]

Photothermally driven volume transitions in polymer hydrogels have promising applications for drug delivery and photodynamic therapy.[5,6] Such transitions are achieved by irradiating microgels carrying photosensitive moieties at the resonance wavelength of the latter. Upon irradiation, the absorption of light and conversion of the light energy to heat through nonradiative relaxation causes heating of microgels in the locally irradiated area and, for polymers with a lower critical solution temperature, results in microgel deswelling. When a drug is loaded in the microgel interior, the shrinkage can cause release of the drug from the microgel carrier.[7] For applications in drug delivery, it is imperative to conduct irradiation in the "water window", that is, in the spectral range 800 nm < λ < 1200 nm.[8]

Recently, our group has reported photothermally triggered reversible deswelling of microgels loaded with gold nanorods (NRs) that were designed to absorb near-IR light. At neutral pH, the NRs were loaded in poly(*N*-isopropylacrylamide-acrylic acid) (poly(NIPAm-AA) microgels by using attractive interactions between the positively charged NRs and the negatively charged AA groups. At pH = 4.0, following irradiation at λ = 809 nm, hybrid microgels underwent a volume transition at 34 °C. These temperature and pH values did not correspond to the physiological conditions of pH = 7.4 and the temperature of 37−41 °C. In fact, at pH = 7.4, no transition up to 60 °C was observed for poly-(NIPAm-AA) microgels containing AA in concentrations as small as 3 mol %: a very small amount of AA in the microgels caused a large shift in the volume phase-transition temperature (VPTT).

Here, our objective was to develop a microgel system that, upon loading with gold NRs, undergoes a photothermally induced volume transition in physiological conditions. We defined the following criteria for the hybrid microgels to be used as the drug carriers:

(a) The temperature-induced deswelling of microgels must occur in the physiologically relevant range: in the temperature range of 38−41°C and at pH = 7.4 in buffer conditions.

(b) The extent of deswelling of microgels at the VPTT must be sufficiently large to trigger the release of a drug loaded in the microgel interior.

(c) To sequester positively charged NRs, microgels should contain negatively charged functional groups.

(d) The NRs should remain within the microgels when subjected to repeated irradiation-triggered swelling−deswelling transitions.

(e) The dispersions of microgels loaded with NRs should be stable in the physiological environment and upon cyclical heating and cooling.

In the present paper, we report several approaches to polyNIPAm-based microgels that include (i) the synthesis of microgels with an interpenetrating (IPN) network structure, (ii) counterbalancing the hydrophilicity of charged acidic groups by copolymerizing NIPAm and AA with a hydrophobic monomer, and (iii) copolymerization of NIPAm with different types of acidic monomers that temper the hydrophilic/hydrophobic properties of the microgels.

† Part of the Stimuli-Responsive Materials: Polymers, Colloids, and Multicomponent Systems special issue.

* Corresponding author.

(1) Pelton, R. *Adv. Colloid Interface Sci.* **2000**, *85*, 1−33.

(2) (a) Mohan, R.; Ramanan, K.; Chellamuthu, P.; Tang, L.; Nguyen, K. *Biotechnol. Prog.* **2006**, *22*, 118−125. (b) Kidane, A.; Bhatt, P. P. *Curr. Opin. Chem. Biol.* **2005**, *9*, 347−351. (c) Hoffman, A. S. *J. Controlled Release* **1987**, *6*, 297−305. (d) Huang, G.; Gao, J.; Hu, Z.; St. John, J. V.; Ponder, B. C.; Moro, D. *J. Controlled Release* **2004**, *94*, 303−311.

(3) Zhang, H.; Mardyani, S.; Chan, W. C. W.; Kumacheva, E. *Biomacromolecules* **2006**, *7*, 1568−1572.

(4) Das, M.; Mardyani, S.; Chan, W. C. W.; Kumacheva, E. *Adv. Mater.* **2006**, *18*, 80−83.

(5) Thurmond, K. B., II; McEwan, J.; Moro, D. G.; Rice, J. R.; Russell-Jones, G.; St. John, J. V.; Sood, P.; Stewart, D. R.; Nowotnik, D. P. *ACS Symp. Ser.* **2006**, *923*, 137−154.

(6) Gorelikov, I.; Field, L. M.; Kumacheva, E. *J. Am. Chem. Soc.* **2004**, *126*, 15938−15939.

(7) Sershen, S. R.; Westcott, S. L.; Halas, N. J.; West, J. L. *J. Biomed. Mater. Res.* **2000**, *51*, 293−298.

(8) Simpson, C. R.; Kohl, M.; Essenpreis, M.; Cope M. *Phys. Med. Biol.* **1998**, *43*, 2465−2478.

10.1021/la061596s CCC: $37.00
Published on Web 10/17/2006

Table 1.

series	microgel composition	NIPAm (mol × 10^3)	NIPMAm (mol × 10^3)	AA (mol × 10^{-4})	BMA (mol × 10^{-3})	UA (mol × 10^{-4})	MA (mol × 10^{-4})	PAA (mol × 10^{-4})	KPS (mol × 10^{-4})	BIS (mol × 10^{-4})	mol % acid	*D* (nm)	transition range (°C)
A	NIPAm	12.5							1.7			124	32−40
B1	poly(NIPAm-BMA-AA)	4.1		1.3	8.4				1.9	3.4	2.0		27−52
B2	poly(NIPAm-BMA-AA)	4.1		1.7	8.4				1.9	3.4	3.0		27−52
B3	poly(NIPAm-BMA-AA)	4.1		3.3	8.4				1.9	3.4	4.0		24−48
B4	poly(NIPAm-BMA-AA)	4.1		8.3	8.4				1.9	3.4	8.0		
U1	poly(NIPAm-UA)	7.8				4.2			2.2	3.4	5.0	427	27−33
U2	poly(NIPAm-UA)	4.2				4.2			2.2	3.4	10.0	538	23−35
U3	poly(NIPAm-UA)	2.4				4.2			2.2	3.4	15.0	567	21−32
U4	poly(NIPMAm-UA)		7.9			4.2			2.2	3.4	5.0	272	39−46
U5	poly(NIPMAm-UA)		3.7			4.2			2.2	3.4	10.0	301	37−43
U6	poly(NIPMAm-UA)		2.1			4.2			2.2	3.4	15.0	359	33−45
M1	poly(NIPAm-MA)	8.0					4.2		2.2	3.4	5.0	414	31−33
M2	poly(NIPAm-MA)	4.2					4.2		2.2	3.4	10.0	624	38−40
M3	poly(NIPAm-MA)	2.4					4.2		2.2	3.4	15.0	671	40−44
N2	poly(NIPAm-NIPMAm)	4.4	5.5						2.2	3.4		776	37−41
IPN3	poly(NIPAm-NIPMAm)/PAA	3.5	3.1					1.0	2.2	3.4		255	35−42
IPN4	poly(NIPAm-NIPMAm)/PAA	2.7	3.9					1.0	2.2	3.5		266	38−45

Experimental

Materials. *N*-Isopropylacrylamide (NIPAm), *N*-isopropylmethacrylamide (NIPMAm), maleic acid (MA), undecanoic acid (UA), butyl methacrylate (BMA), poly(acrylic acid) (PAA, $M_w = 2000$ g/mol), a cross-linking agent *N*-*N*′-methylene-bis-acrylamide (BIS), and an initiator potassium persulfate (KPS) were purchased from Aldrich Chemical Co. (Canada) and used as received.

Synthesis of Microgels. The recipes used for microgel synthesis are given in Table 1. All microgels were prepared via free radical precipitation polymerization. An aqueous solution (90 mL) containing NIPAm, respective comonomers, and BIS was placed in a 250 mL jacketed round-bottomed flask equipped with a N_2 inlet. The solution was mechanically stirred at 300 rpm under nitrogen for 1 h and then heated to 70 °C. At this point, 10 mL of 5 wt % KPS solution were injected in the flask. The proportions of reactants in various reaction mixtures are given in Table 1. Following synthesis, the microgels were purified several times by centrifugation (10 000 rpm, 30 min at 4°C) and redispersed in a buffer solution at pH = 7.4.

For the synthesis of poly(NIPAm-UA) microgels, prior to injection in the reaction mixture, UA was first reacted with NaOH to yield the water-soluble salt form. For the preparation of poly(NIPAm-NIPMAm)-PAA IPN microgels, prior to the synthesis of microgels, PAA was added to the aqueous reaction mixture.

Preparation of Microgels Doped with Gold NRs. Gold NRs were synthesized following the procedure developed by Nikoobakht and El Sayed,[9] and were scaled up to obtain a 100 mL dispersion of the NRs. Gold seed nanoparticles were prepared by reducing $HAuCl_4$ (0.12 mL, 5 mM) mixed with 2.5 mL of an aqueous 0.2 M cetyl trimethylammonium bromide (CTAB) with sodium borohydride (0.5 mL, 10 mM) in ice-cold water. For the preparation of a growth solution, 25 mL of a 0.2 M CTAB solution were mixed with 25 mL of a 0.2 M benzyldimethylhexadecylammonium chloride solution. To this solution, 5 mL of an aqueous 5 mM solution of $HAuCl_4$, 2.8 mL of an aqueous 4 mM $AgNO_3$ solution, and 40 mL of water were added. Upon the addition of 1 mL of a 0.8 M aqueous solution of ascorbic acid, the dark yellow solution turned colorless. Finally, we added 1 mL of 5-min-aged seed solution to the growth solution. This route allowed for the preparation of gold NRs with plasmon bands centered at ∼840 nm. The NRs were purified via three 30-min-long centrifugation cycles at 10 000 rpm. At the end of each centrifugation cycle, the supernatant was removed, and the precipitated NRs were redispersed in deionized (DI) water. Microgels were loaded with NRs by mixing the purified microgel and NR dispersions under continuous stirring in the ratio of 2:1, respectively.

Characterization of Microgel Properties. Variation in microgel size as a function of temperature was measured using a photon correlation spectroscopy (PCS) setup (Protein Solutions, Inc.) equipped with a temperature controller. All measurements were conducted in phosphate-buffered saline (PBS) at pH = 7.4 unless otherwise specified. The electrophoretic mobility of the microgels was measured on a Zetasizer 3000HS (Malvern Instruments).

Photothermally triggered change in microgel size was measured using a PCS setup at 632.8 nm (Zetasizer 3000HS, Malvern Instruments), modified to accommodate the pump laser. The hybrid microgels dispersed in PBS buffer at pH = 7.4 were heated to 36 °C and then irradiated at $\lambda = 809$ nm (surgical laser CW/pulsed, 1.5 W power). The temperature of the microgel dispersion was monitored with a thermocouple probe placed inside the cuvette.

Loading of microgels with NRs was examined by scanning transmission electron microscopy (TEM) (Hitachi HD 2000). The composition of the microgels with an IPN network structure was verified by Fourier transform infrared (FTIR) spectroscopy. Samples of the microgels in an acid form were dried in air and embedded in KBr pellets. Experiments were carried out using a Perkin-Elmer PARAGON 500 FTIR instrument. Each sample was analyzed between 400 and 4000 cm^{-1}, at 32 scans and a resolution of 4 cm^{-1}.

Results

We carried out several series of experiments to find the system that best satisfied the criteria outlined above. For each microgel system, we verified the temperature range and the sharpness of the temperature-induced transitions. The results of these experiments are presented in Table 1. The best representative results for each of the microgel series are given in Figure 1, along with the result for the reference system. Microgels with promising properties (based on the criteria described above) were loaded with NRs and examined under TEM. Photothermally induced volume transitions for hybrid microgels were tested only for the system with the best performance.

Copolymerization of NIPAm with Different Acidic Functionalities. *Copolymerization of NIPAm with UA.* We examined the effect of copolymerization of NIPAm with UA on the onset of microgel deswelling and the sharpness of the VPTTs. We built our work on the results of Yang et al.,[10] who found no change in the lower critical solution temperature of NIPAm for the linear copolymer of NIPAm and UA.

We copolymerized NIPAm with UA in various compositions (Table 1, series U1−U3) and examined the VPTTs of the corresponding microgels in buffer at pH = 7.4. Table 1 shows the change in the hydrodynamic radius of a microgel with different fractions of UA as a function of temperature. The best result was

(9) Nikoobakht, B.; El-Sayed, M. A. *Chem. Mater.* **2003**, *15*, 1957−1962.

(10) Soppimath, K. S.; Tan, D. C.-W.; Yang, Y.-Y. *Adv. Mater.* **2005**, *17*, 318−323.

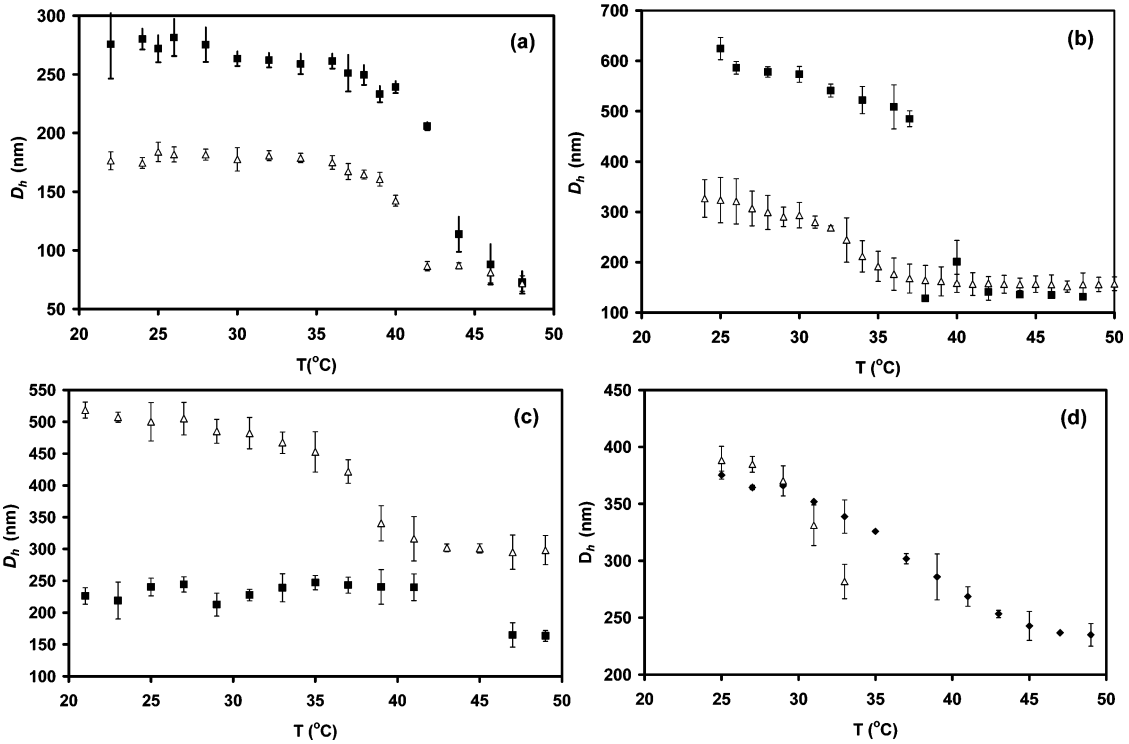

Figure 1. Variation in the hydrodynamic diameter of microgels as a function of temperature in PBS, pH = 7.4: (a) polyNIPMAm-UA (series U4) (■) and poly(NIPMAm) (△) microgels; (b) polyNiPAm-MA (■) and poly(NIPAm) (△) microgels; (c) poly(NiPAm-NIPMAm)/PAA IPN (■) and poly(NIPAm-NIPMAm) (△) microgels. (d) poly(NiPAm-AA-BMA) (■) and poly(NIPAm-BMA) (△) microgels. In panel d, the heating of poly(NIPAm-BMA) microgels above 33 °C caused particle coagulation.

achieved for the microgels of series U1 synthesized at a [NIPAm]/[UA] molar ratio of 5/100 in the reaction mixture. These microgels underwent a 95% reduction in volume in the temperature range of 27−45 °C, with 39% of the shrinkage occurring between 27 and 33 °C. However, the shrinkage between 38 and 41 °C was negligible. The hydrophobicity of the undecanoic chain nullified any increase in the VPTT due to the hydrophilic COOH groups.[8]

To shift the temperature-induced transition to the target range of 38−41°C, we replaced the NIPAm with NIPMAm. The methyl group on the α-carbon in NIPMAm restricts free rotation of the main chain and inhibits hydrophobic interactions. As a result, the lower critical solution temperature of NIPMAm is 42−44 °C, almost 10 °C higher than that of NIPAm. Poly(NIPMAm-UA) microgels of different compositions showed VPTTs in the range of 27−35 °C (Table 1). In particular, Figure 1a shows that poly-(NIPMAm-UA) microgels containing 5 mol % UA (Series U4) underwent a 91% reduction in volume between 39 and 41°C. The broader transition range of poly(NIPMAm-UA) microgels compared to that of poly(NIPAm-UA) microgels was attributed to the greater hydrophilicity of the former, as follows from the variation in the hydrodynamic radius of polyNIPMAm microgels with temperature (Figure 1a).

Copolymerization of NIPAm with MA. Since the transition temperature of polyNIPAm depends on the conformational arrangement of water molecules around the amide residues,[11] the interruption of polyNIPAm chain segments by other functional groups typically results in deviation from, and broadening of, the VPTT of polyNIPAm.[12] By contrast, incorporation in the polymer chains of multifunctional ionic groups increases the net charge density, magnifying the change in size during the swelling−deswelling transition of the microgel while introducing fewer interruptions in the NIPAm chain segments that are otherwise responsible for large deviations from the VPTT.[13]

We modulated the VPTTs of microgels by copolymerizing NIPAm with MA, a diprotic carboxylic acid with two pK_a's of 1.9 and 6.08. [13] Several representative results for this system are shown in Table 1 (series for Figure 1b shows the thermally induced transition of polyNIPAm (reference system) and poly-(NIPAm-MA) microgels polymerized at a molar ratio of [MA]/[NIPAm] in the reaction mixture of 10/90. As a reference system, we plotted the variation in hydrodynamic diameter of polyNIPAm microgels. The former system displayed an ∼74% decrease in diameter of microgel particles in the desired temperature range from 38 to 41 °C at pH = 7.4, which translated to an ∼98% change in volume of the microgels. Note the negligible change in microgel size at 37 °C (at normal body temperature), the narrow temperature range of the volume transition, and the large (almost 8-fold) decrease in microgel size.

Microgels with IPN Network Structures. While the copolymerization of acidic functionalities with NIPAm is an effective route to tuning the VPTTs of microgels, the varying reactivity of the monomers limits control over the final composition of microgels and the distribution of functional groups within the particles. These features influence the swelling behavior of microgels.[14] We explored an alternative method for incorporating acidic functional groups in the microgels by preparing microgels from two polymers physically bonded into an IPN structure. Hu and Xia showed that, for polyNIPAm/PAA IPN microgels, there are two primary advantages of using IPNs over randomly copolymerized microgels: the facile incorporation of a large

(11) Schild, H. G. *Prog. Polym. Sci.* **1992**, *17*, 163−249.
(12) Wu, C.; Zhou, S.; Au-yeung, S. C. F.; Jiang S. *Angew. Makromol. Chem.* **1996**, *240*, 123−136.
(13) Malik, R. A.; Solis, F. J.; Vernon, B. L. *J. Appl. Polym. Sci.* **2004**, *94*, 2110−2116.
(14) (a) Ogawa, Y.; Ogawa, K.; Kokufuta, E. *Langmuir* **2004**, *20*, 2546−2552. (b) Ogawa, K.; Ogawa, Y.; Kokufuta, E. *Colloids Surf., A* **2002**, *209*, 267−279. (c) Kokufuta, E.; Wang, B.; Yoshida, R.; Khokhlov, A. R.; Hirata, M. *Macromolecules* **1998**, *31*, 6878−6884.

number of functional groups within the particle, and no shift in the VPTT of polyNIPAm.[15]

In the present work, the targeted VPTT range was achieved by polymerizing one of the polymers of IPN from a copolymer of NIPAm and NIPMAm. The IPN microgels were obtained by copolymerizing NIPAm and NIPMAm in the presence of PAA. Presence of PAA in the microgels was confirmed by FTIR measurements that showed a new band at 1738 cm^{-1}, characteristic for absorption by carboxylic groups.[16] In addition, the ζ potential of the poly(NIPAm-NIPMAm) IPN microgels was −18 mV (vs only several millivolts for poly(NIPAm-NIPMAm) microgels). Increasing the concentration of PAA in microgels led to a decrease in microgel size, in contrast with earlier observations by Hu and Xia.[17] At the moment, we are unable to explain the difference. However, we speculate that both the significantly lower molecular weight of the PAA used in the present work and the use of a different synthetic procedure from that used by Hu et al. may be responsible for the different observations. Furthermore, the smaller size of IPN microgels in comparison with the corresponding poly(NIPAm-NIPMAm) microgels may be due to the formation of microdomains resulting from hydrophobic interactions between short PAA chains and poly(NIPAm) segments in the network.[14b] For all IPN microgels, irrespective of PAA content in the particles, no shift in VPPT was observed in comparison with the host poly(NIPAm-NIPMAm) microgels.

Figure 1c shows the variation in the size of poly(NIPAm-NIPMAm) microgels synthesized at a [NIPAm]/[NIPMAm] molar ratio of 41/59 and that for the corresponding IPN poly-(NIPAm-NIPMAm)-PAA microgels. The poly(NIPAm-NIPMAm)/PAA IPN microgels shrank from ∼250 to ∼150 nm in the temperature range of 41−47 °C, corresponding to an ∼78.4% decrease in volume. The deswelling ratio of poly(NIPAm-NIPMAm)/PAA IPNs was lower than that of pure poly(NIPAM) microgels.

Copolymerization with a Hydrophobic Comonomer. Generally, copolymerization of NIPAm with a more hydrophobic monomer moves the onset of microgel shrinkage to lower temperatures. For example, Feil et al.[18] showed that the microgels synthesized from NIPAm, AA, *and* BMA had volume phase transition temperatures in the temperature range of 35−40 °C in PBS solution of pH = 7.4. These results showed that the higher values of volume phase transitions in poly(NIPAm-AA) caused by the hydrophilic nature of the AA at pH = 7.4 were counterbalanced by the hydrophobic nature of BMA.

Here, we synthesized poly(NIPAm-BMA-AA) microgels at a constant molar ratio [NIPAm]/[BMA], while the content of AA in the reaction mixture varied from 2 to 8 mol %. The recipes used for the microgel syntheses are given in Table 1 (series B1−B4). The initial size of poly(NIPAm-AA-BMA) microgels and the temperature of the volume transition increased with increasing AA content in the reaction mixture. On the other hand, with increasing concentration of AA, the extent of shrinkage of microgels as a function of temperature decreased. The VPTTs were broad and occurred over the temperature range of ∼8−10 °C; however, unlike that for poly(NIPAm-AA) microgels, all VPTTs started well below 60 °C.

Figure 1d shows the variation in the hydrodynamic diameter of poly(NIPAm-BMA-AA) microgels (series B1, Table 1) with the VPTT closest to the desirable temperature range. As a reference, on the same graph we show the deswelling behavior of poly(NIPAm-BMA) microgels. In the temperature range of 25−50 °C, the change in the diameter of poly(NIPAm-BMA-AA) microgels was ∼130 nm, that is, approximately 13% of the original microgel size, with 11% shrinkage occurring between 38 and 41 °C. The reference poly(NIPAm-BMA) microgels coagulated at 33 °C. We attribute the breadth of the deswelling transition and the poor shrinkage of poly(NIPAm-BMA-AA) microgels to the presence of BMA: the higher hydrophobicity of BMA may cause it to segregate toward the center of the microgel, increasing the rigidity of the polymer and thus reducing the overall extent of microgel shrinkage.

We note that, for microgels of series B1 and B2 (Table 1) with 2 and 3 mol % of AA, notable shrinkage started at ∼35 °C, whereas, for series 3 and 4, the transition began at 41 °C. Thus, in principle, by tuning the concentration of AA, the onset of the transition may be shifted to the desired range of 38−41 °C. Nevertheless, the breadth of the VPTTs did not make this approach promising in view of our listed criteria.

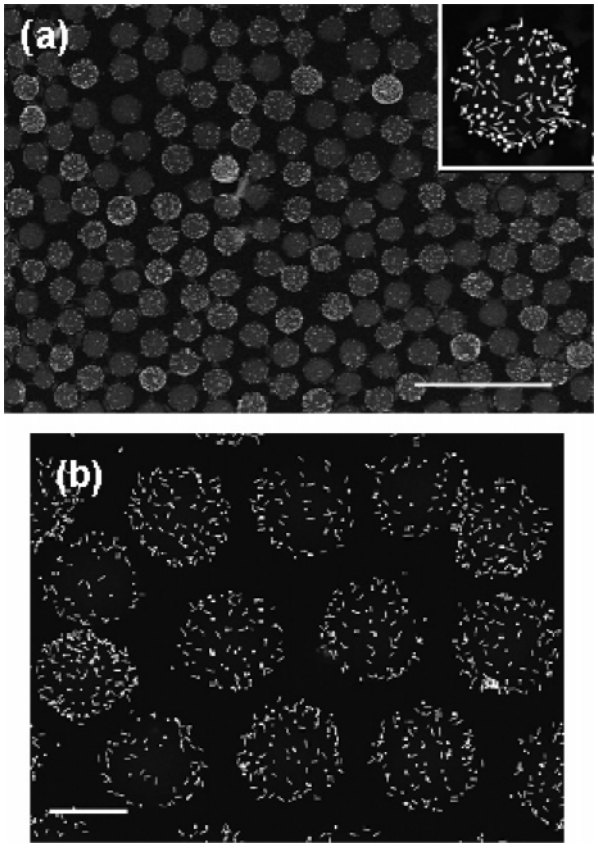

Figure 2. Typical TEM images of microgels loaded with gold NRs. (a) Poly(NIPAm-MA) microgels (as in Figure 1b). Scale bar is 2 μm. Inset shows a single 200 nm microgel particle loaded with NRs. (b) Poly(NIPAm-NIPMAm)/PAA microgels (as in Figure 1c). Scale bar is 400 nm.

Incorporation of NRs in the Microgels. We selected the two most promising systems, namely, poly(NIPAm-MA) microgels (series M2) and poly(NIPAm-NIPMAm)/PAA IPN microgels (Series IPN4), to explore the incorporation of NRs in the microgel interior. Figure 2a,b shows TEM images of the poly(NIPAm-MA) microgels and of poly(NIPAm-NIPMAm)/PAA IPN microgels loaded with gold NRs, respectively. All the NRs were loaded on the microgels, while an extremely small amount of NRs was observed in the free interstitial space. Within the microgels, a homogeneous distribution of NRs within the microgels was observed for both systems.

(15) Xia, X.; Hu, Z.; Marquez, M. *J. Controlled Release* **2005**, *103*, 21−30.
(16) Hyk, W.; Ciskowqka, M. *J. Phys. Chem. B* **2002**, *106*, 11469−11473.
(17) Xia, X.; Hu, Z. *Langmuir* **2004**, *20*, 2094−2098.
(18) Feil, H.; Bae, Y. H.; Feijen, J.; Kim, S. W. *Macromolecules* **1993**, *26*, 2496−2500.

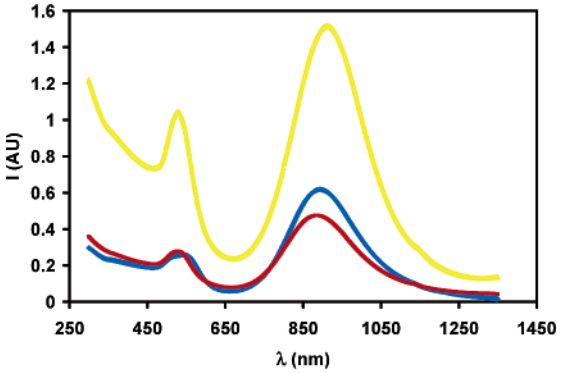

Figure 3. Absorption spectra of gold NRs prior to (black line) and following NR incorporation in poly(NIPAm-MA) (yellow line) and poly(NIPAm-NIPMAm)-PAA IPN4 (red line) microgels.

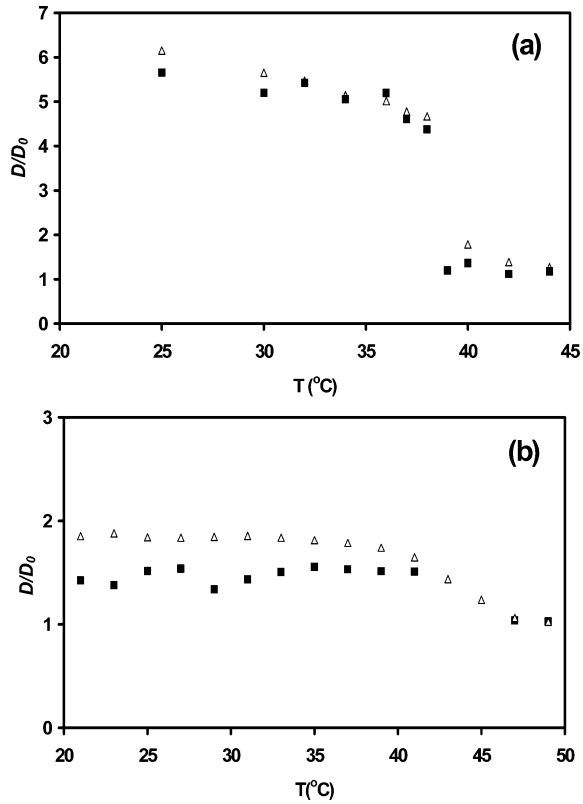

Figure 4. Variation in the deswelling ratios, D/D_0, of NR-free (△) and NR-loaded (■) microgels: (a) poly(NIPAm-MA) microgels (series M2, Table 1) in PBS at pH = 7.4; (b) poly(NIPAm-NIPMAm)/PAA IPN microgels (series IPN4, Table 1) in DI water. D and D_0 are the hydrodynamic diameters of the corresponding microgels at the temperature of interest and at room temperature, respectively, in buffer solution at pH = 7.4.

We further tested the absorption properties of gold NRs following their loading in the interior of poly(NIPAm-MA) and poly(NIPAm-NIPMAm)/PAA microgels (as in Figure 2). Figure 3 shows that, for both systems, the absorption properties of the gold NRs did not change significantly upon incorporation within the microgel interior. A slight (up to 20 nm) red shift was caused by the change in the dielectric constant of the environment surrounding the NRs.

Following the incorporation of NRs in the microgels, we examined temperature-induced variations in the size of hybrid poly(NiPAm-MA) and poly(NIPAm-NIPMAm)/PAA IPN microgels. Figure 4 shows the relative change in microgel size, D/D_0, where D_0 is the hydrodynamic diameter of the corresponding microgel.

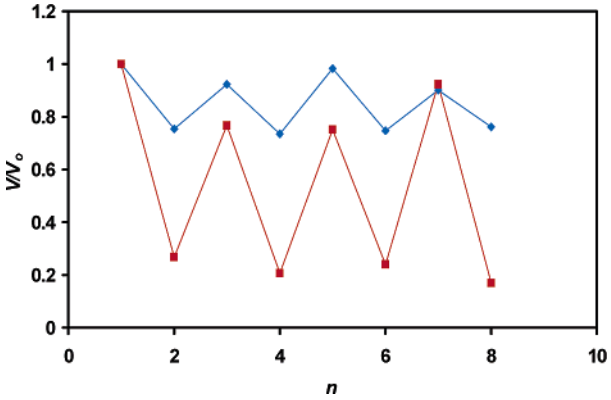

Figure 5. Variation in deswelling ratio, V/V_0, as a function of the number of *laser-on* and *laser-off* events for pure (◆) and hybrid (■) poly(NIPAm-MA) microgels (series M2). V_0 is the volume of the microgel at 25 °C; V is the volume of the microgel following irradiation.

Figure 4a shows the deswelling behavior of NR-free and hybrid poly(NiPAm-MA) in buffer solution at pH = 7.4. At 25 °C, the doped poly(NiPAm-MA) microgels were ∼7% smaller in diameter than NR-free microgels. This difference, though very small, was attributed to the higher ionic strength of the hybrid system and the physical cross-linking of the microgel particles with the gold NRs. Upon heating, the hybrid microgels shrank to a slightly smaller size; however, the relative size change of pure and hybrid microgels was very similar. The VPTT of hybrid poly(NiPAm-MA) particles remained very similar to that of NR-free microgels. The transition occurred in the targeted range of 38−41 °C.

By contrast, hybrid poly(NIPAm-NIPMAm)/PAA IPN microgels coagulated in a PBS buffer when heated above 40 °C. Therefore, the behavior of NR-loaded IPN microgels was examined in water at pH = 7.0. Figure 4b shows the variation in the deswelling ratio D/D_0 of NR-free and NR-loaded poly(NIPAm-NIPMAm)/PAA microgels. The trends were similar to those shown in Figure 4a: a slightly smaller size of hybrid microgel and a very similar deswelling behavior of pure and hybrid microgels. However, the extent of shrinkage of hybrid IPN microgels was significantly smaller than that of the poly(NIPAm-MA) microgel.

We further explored the potential applications of the hybrid microgels with respect to their photothermally triggered volume phase transitions. The hybrid poly(NIPAm-MA) microgels dispersed in PBS of pH = 7.4 were heated to 36 °C and repetitively irradiated at λ = 809 nm. The duration of irradiation was approximately a minute, and the time interval between the irradiation cycles was approximately 3 min. In parallel, we measured the temperature of the dispersion. Also, no exact match existed between the irradiation wavelength and the absorbance wavelength of NRs loaded in microgels; following irradiation, we observed a rapid (within a minute) change in particle size. Figure 5 shows the reduction in volume of hybrid poly(NIPAm-MA) microgels doped with gold NRs of 78 ± 4% (that is, about 80% of the volume reduction induced by heating hybrid microgels to 40 °C (Figure 4a). Using the results of steady-state swelling experiments, we estimate the temperature of the microgel particles to be 40 °C. We stress that, following irradiation, the temperature of the bulk dispersion remained at 36 °C.

In contrast, in the control experiment, upon illumination of the dispersion of NR-free microgels at λ = 809 nm, the volume of microgels was reduced by only 25 ± 1%. The strong change in the volume of hybrid microgels resulted from the local heating

of microgels, following conversion of light energy to heat by the gold NRs. The laser-on and laser-off cycles were repeated several times. The photothermally induced deswelling/swelling transitions in hybrid microgels were reproducible, indicating that the NRs remained within the poly (NIPAm-MA) microgels during the heating cycles.

Discussion

Our results show that various routes can be used to tune the volume phase transition temperature of NIPAm-based microgels. Modulating hydrophilic/hydrophobic balance of microgels by polymerizing suitable comonomers is a seemingly straightforward approach. However, the differences in reactivities of the comonomers and different solubilities of the corresponding polymer molecules may result in a nonuniform polymer composition throughout the microgel. Copolymerization of NIPAm with hydrophobic monomers reduces the extent of shrinkage, while copolymerization with hydrophilic monomers broadens the temperature range of the deswelling transition. Microgels with IPN network structures provide a promising alternative for the incorporation of functional groups in thermoresponsive microgels without affecting the temperature of volume transition. In the present work, however, IPN microgels showed a limited stability to coagulation at elevated temperatures and a small magnitude of volume transition.

Among all systems studied, copolymerization of NIPam with MA produced microgels that satisfied all the criteria defined in the Introduction. The diprotic MA introduced twice the number of charged groups with half the number of interruptions in the poly(NIPAm) segments compared to the AA used in our previous work.[6] The increase in the VPTT of poly(NIPAm-MA) microgels to 38 °C (in comparison with 32 °C for polyNIPAm) was what caused the hydrophilicity of the MA at pH = 7.4. Poly(NIPAm-MA) microgels underwent a massive 98% change in volume between 38 and 40 °C in PBS at pH = 7.4; that is, they featured a significantly stronger deswelling than did polyNIPAm microgels. This large response to thermal stimulus was preserved in hybrid poly(NIPAm-MA) microgels loaded with gold NRs. The poly(NIPAm-MA) microgels were stable in the temperature range studied in the present work.

At the moment, we are unable to address the question about the distribution of MA in the microgels, as well as the localization of NRs in the particles. However, we stress that, regardless of whether the NRs were localized in the microgel interior or at the periphery of the particles, the reversibility of the photothermally triggered deswelling of hybrid microgels indicated sufficiently strong interactions between the microgels and the NRs. Poly(NIPAm-MA) microgels can be bioconjugated to make them suitable for site-specific drug delivery.[3,4] Incorporation of small molecules and drugs in the microgel interior and their photothermally triggered release is the next logical step of this work. Finally, the approach described in the present work can be applied to microgels formed by biopolymers with a lower critical solution temperature.

LA061596S